JOURNAL OF MATERIALS SCIENCE **32** (1997) 4283–4287

Effect of chromium on the phase evolution and microstructure of ZnO doped with bismuth and antimony

SUNG GURL CHO, HOON LEE*
Departments of Inorganic and Electronic Materials Engineering and Research Center for Aircraft Parts Technology, Gyeongsang National University, Chinju, Gyeongnam 660-701, Korea*

HYUNG SIK KIM
Korea Electrotechnology Research Institute, Changwon, Gyeongnam 641-120, Korea

Crystalline phase formation and microstructure of ZnO varistors with a basic composition ZnO–Bi_2O_3–Sb_2O_3 were examined. Addition of chromium oxide to this basic varistor resulted in an α-spinel (α-$Zn_7Sb_2O_{12}$) phase dissolving a significant amount of Cr, while the β-spinel did not. β-spinel transformed to pyrochlore during cooling, whereas α-spinel hardly transformed to pyrochlore irrespective of the cooling conditions. When Sb_2O_3 was completely replaced by Cr_2O_3, $ZnCr_2O_4$ was formed instead of spinel. α-spinel particles were 1–2 μm in size and intra- as well as intergranular. $ZnCr_2O_4$ particles, smaller than 1 μm in size, however, were present as aggregates in the bismuth-rich matrix phase at the grain boundaries.

1. Introduction

ZnO varistors have been widely used for protection devices for small current electronic circuits as well as for large current transmission lines. Electrical properties, microstructures and electric conduction mechanisms of ZnO varistors have been investigated by many researchers [1–4]. However, the role of each component during sintering is not clearly understood. There have been investigations of the sintering and microstructure of basic ZnO varistor compositions [5], and further studies on ZnO–Bi_2O_3 [6], ZnO–Sb_2O_3 [7, 8] binary and ZnO–Bi_2O_3–Sb_2O_3 [9] ternary systems were reported recently.

In the ZnO–Bi_2O_3–Sb_2O_3 ternary [9], densification was found to be dependent on the Sb/Bi ratio that determines the temperature at which the liquid (L) phase is formed during sintering. When the Sb/Bi ratio is smaller than unity, the liquid phase is formed at the melting temperature of Bi_2O_3. When the Sb/Bi ratio, however, is larger than unity, the liquid phase is introduced at the temperature that the pyrochlore phase decomposes to spinel and Bi_2O_3(L) at about 1000 °C. It is important to know which crystalline phase is present during sintering to understand the microstructural evolution of ZnO varistors, because spinel and pyrochlore are known to be responsible for grain-growth inhibition, while a liquid phase promotes grain growth during sintering [2, 9].

The aim of this study is to understand the effect of chromium on the microstructure of ZnO varistors. The crystalline phases and microstructures of ZnO–Bi_2O_3–Sb_2O_3 ternary compositions were examined prior to investigating those of ZnO–Bi_2O_3– Sb_2O_3–Cr_2O_3 quarternary compositions to clarify the effect of chromium.

2. Experimental procedure

Chemical compositions without Cr were $(99.0 - x)$% ZnO, 1.0% Bi_2O_3 and x% Sb_2O_3 ($x = 0, 0.3, 0.5, 0.7$), while those containing Cr were 98.0% ZnO, 1.0% Bi_2O_3 and 1.0% ($Sb_2O_3 + Cr_2O_3$) with varying Cr; 0, 0.3, 0.5, 0.7 and 1.0% (all compositions are in mol%).

Conventional mixed oxide ceramic processing was used to prepare specimens. Reagent grade ZnO, Bi_2O_3, Sb_2O_3 and Cr_2O_3 were mixed using a ball mill with methanol and zirconia balls. The powder was granulated by passing through a sieve after mixing with polyvinyl alcohol (PVA) solution using an alumina mortar and pestle. Disc-shaped green compacts with diameters of 15 mm were uniaxially pressed and sintered at 1100 °C for 1 h in an ambient atmosphere. Basically, sintered specimens were cooled in the furnace that was shut off after completion of the soak time. Some specimens, however, were slowly cooled at 2 °C min^{-1} or quenched in air to examine the effect of cooling rate on the phase transformation.

Apparent densities of all sintered specimens were measured to check the degree of densification. The fracture surfaces of the specimens were polished and chemically etched with 0.5% HF aqueous solution to

0022–2461

examine the microstructure using an optical microscope (Nicon Epiphoto-TME) or a scanning electron microscope (SEM, Jeol JSM-6400). Average grain sizes of the specimens were measured using the linear intercept method from optical micrographs. The second phase present within grains or grain boundaries were investigated using energy dispersive X-ray analysis (EDX, Noran EDX Series II), while crystalline phases of the sintered specimens were analysed using X-ray diffraction (XRD) analysis (Rigaku D/MAX-3C) and JCPDS cards (ZnO, 5-664; β-Bi_2O_3, 27-50; δ-Bi_2O_3, 27-52; β-$Zn_7Sb_2O_{12}$, 36-1445; and $ZnCr_2O_4$, 22-1107). Because XRD data for α-$Zn_7Sb_2O_{12}$ and pyrochlore were not found in the JCPDS cards, XRD patterns presented in published papers were used [6, 7, 10]. The degree of contact, or the contiguity, of the grains was measured to compare wettability of the liquid phase during sintering for the specimens with different compositions.

The contiguity can be expressed as [11]

$$C_{zz} = \frac{4(P_L)_{zz}}{4(P_L)_{zz} + 2(P_L)_{zl}} \qquad (1)$$

where $(P_L)_{zz}$ and $(P_L)_{zl}$ are the number of intersections per unit length, L, of test line with ZnO/ZnO and ZnO/liquid phase interface traces, respectively. $(P_L)_{zz}$ and $(P_L)_{zl}$ were measured from the SEM micrographs obtained for the specimens quenched at sintering temperature.

3. Results and discussion

3.1. ZnO–Bi_2O_3–Sb_2O_3

The average grain size of the sintered specimens with different amounts of antimony oxide is shown in Fig. 1. As is well known, addition of antimony oxide decreases ZnO grain size. However, the grain size reduction was not strongly dependent on the amount of antimony oxide added being ~15 μm for amounts from 0.3 to 1 mol %.

X-ray diffraction patterns of the sintered specimens given in Fig. 2 show spinel (β-$Zn_7Sb_2O_{12}$), pyrochlore ($Bi_{3/2}ZnSb_{3/2}O_7$) and bismuth oxide (β-Bi_2O_3) phases besides ZnO as reported by numerous researchers [2, 4, 9]. Because the maximum peak of β-spinel and the second largest peak of β-Bi_2O_3 overlap at $2\theta \approx 33°$, the peak height of the β-Bi_2O_3 maximum at $2\theta \approx 28°$ is considered to determine the relative amount of β-spinel. The variation of crystalline phases obtained for different compositions must be a function of the reactions during sintering and cooling. Inada [4] suggested that bismuth oxide, antimony oxide and zinc oxide react to form pyrochlore above 900 °C, and the pyrochlore reacts with zinc oxide to decompose into spinel and bismuth oxide liquid phase at 950–1050 °C. The reactions will be reversed during cooling depending upon the cooling rate. Phase formation for the samples with 0.5 mol % Sb_2O_3 can be explained as follows: upon heating the starting powder, half of the bismuth oxide reacts with antimony oxide and zinc oxide to form pyrochlore, and the other half of bismuth oxide becomes a liquid phase. Further increase of temperature leads to decomposition of pyrochlore into spinel and bismuth oxide at 950–1050 °C, resulting in a solid spinel phase and liquid bismuth oxide phase at the sintering temperature. Upon cooling, spinel and bismuth oxide react to form pyrochlore. During this reaction all spinel is consumed, hence pyrochlore and bismuth oxide phases are left. Further cooling appears not to lead to decomposition of the pyrochlore, because no antimony oxide peaks were observed in Fig. 2b. Crystalline phases observed at room temperature shown in Fig. 2b agree with the explanation. As the antimony oxide content increased from 0.3 to 1.0 mol %, the bismuth oxide content decreased while pyrochlore increased due to transformation of spinel and bismuth oxide to pyrochlore during cooling (see Fig. 2). The increase of the pyrochlore content as the cooling rate decreases (Fig. 3) confirms that the pyrochlore forms upon cooling.

However, discrepancies from this behaviour were found in samples with 1.0 mol % Sb_2O_3. Because equimolar Sb and Bi exist in the pyrochlore ($Bi_{3/2}ZnSb_{3/2}O_7$), both spinel and bismuth oxide should be either present or absent simultaneously. The presence of β-spinel and absence of bismuth oxide in

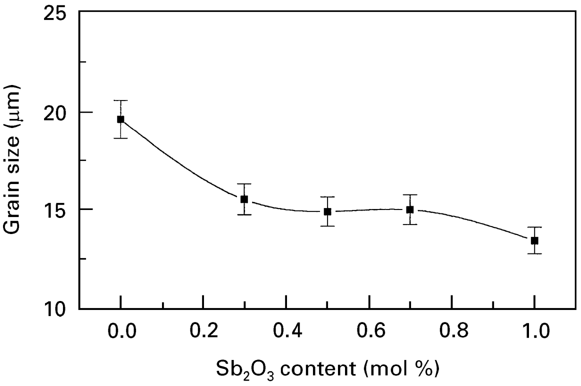

Figure 1 Average grain size as a function of Sb_2O_3 content for ZnO specimens with 1.0 mol % Bi_2O_3 sintered at 1100 °C for 1 h.

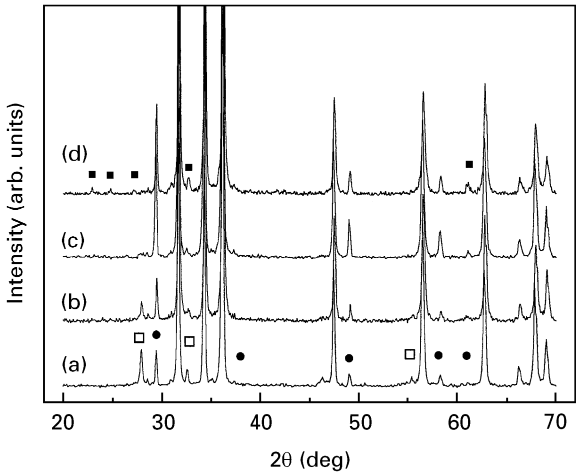

Figure 2 XRD patterns of ZnO specimens sintered at 1100 °C for 1 h that contain 1.0 mol % Bi_2O_3 and various amount of Sb_2O_3: (a) 0.3 mol % Sb_2O_3, (b) 0.5 mol % Sb_2O_3, (c) 0.7 mol % Sb_2O_3, and (d) 1.0 mol % Sb_2O_3. (■) β-$Zn_7Sb_2O_{12}$, (●) pyrochlore, (□) β-Bi_2O_3.

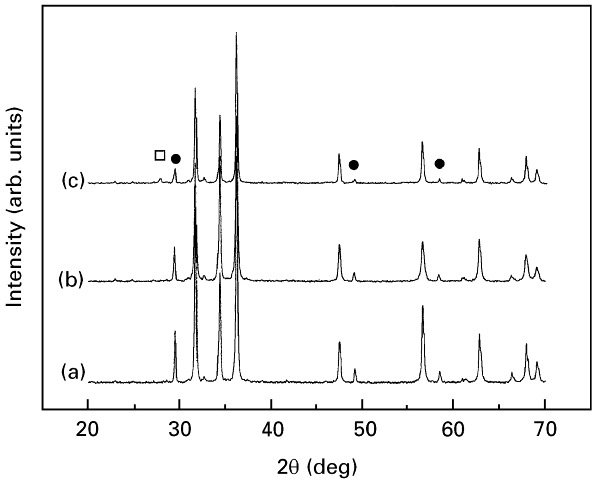

Figure 3 XRD patterns of ZnO specimens sintered at 1100 °C for 1 h that contain 1.0 mol % Bi_2O_3 and 1.0 mol % Sb_2O_3 prepared under different cooling conditions: (a) slow cooling (2 °C min^{-1}), (b) furnace cooling, and (c) quenching. (●) pyrochlore, (□) β-Bi_2O_3.

the samples with 1.0 mol % Bi_2O_3 and 1.0 mol % Sb_2O_3 as shown in Fig. 2d may be attributable to evaporation of bismuth oxide during sintering. Although Inada [4] suggested decomposition of pyrochlore at 950–1050 °C, pyrochlore was detected in the specimen quenched from 1100 °C as shown in Fig. 3c. Kim *et al.* [9] also reported pyrochlore in specimens quenched from 1100 °C. Some pyrochlore remains and is not decomposed to spinel and bismuth oxide during sintering at 1100 °C.

3.2. ZnO–Bi_2O_3–Sb_2O_3–Cr_2O_3

Average grain sizes of the specimens with 1.0 mol % Bi_2O_3 and 1.0 mol % (Sb_2O_3 + Cr_2O_3) as a function of Cr_2O_3 content are given in Fig. 4. It is known that both Sb_2O_3 and Cr_2O_3 inhibit grain-growth of ZnO [4, 12, 13]. Fig. 4 shows, however, that Cr_2O_3 is more effective than Sb_2O_3 in grain-growth inhibition. When Sb_2O_3 was partly or completely replaced by Cr_2O_3, the average grain size was further decreased.

Crystalline phases observed in the samples containing both Sb_2O_3 and Cr_2O_3 were spinel (α-$Zn_7Sb_2O_{12}$) [10], pyrochlore and δ-Bi_2O_3 as shown in Fig. 5. The spinel found in the Cr-containing specimens was α-phase instead of the β-spinel observed in the samples without chromium. The XRD pattern of α-spinel could be distinguished from β-spinel in its relatively large peaks at 2θ ≈29, 35 and 52° [6, 10] and absence of the peaks in the region 2θ = 22–28° [7]. EDX analysis revealed that a significant amount of Cr was dissolved in the α-spinel phase. Also the shift of α-spinel peaks with chromium oxide content observed in Fig. 5 suggests dissolution of Cr in the spinel. Therefore, it can be concluded that dissolution of chromium in the spinel, presumably replacing Sb ions, is responsible for α-spinel stabilization. The Bi_2O_3 phase present in the Cr-containing samples was the δ-phase instead of the β-Bi_2O_3 observed in the specimens without Cr. Although a combination of β-phase and δ-phase was reported for the composition more complicated than that used in this study [13], only δ-Bi_2O_3 was identified.

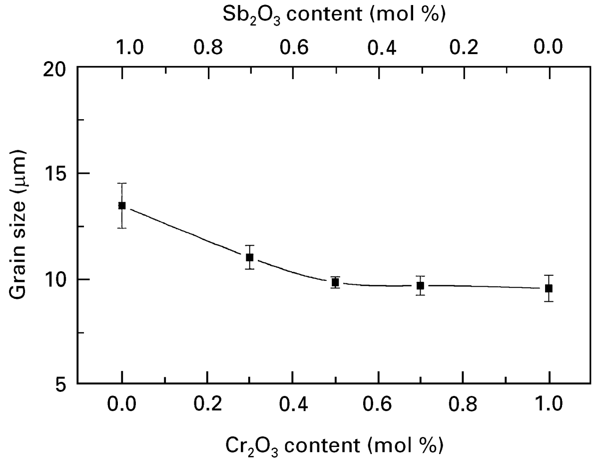

Figure 4 Average grain size as a function of Cr_2O_3 content for ZnO specimens sintered at 1100 °C for 1 h that contain 1.0 mol % Bi_2O_3 and 1.0 mol % (Sb_2O_3 + Cr_2O_3).

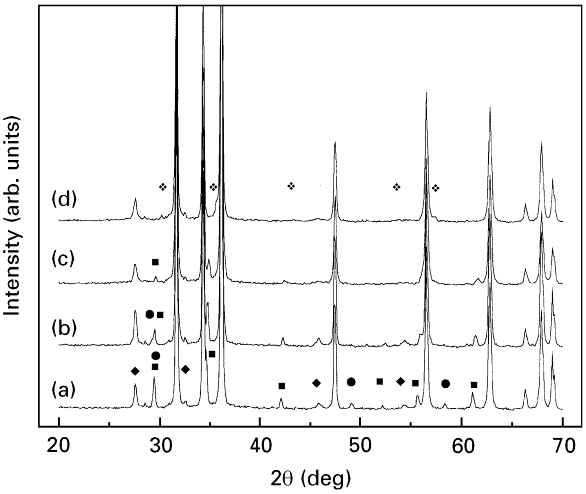

Figure 5 XRD patterns of ZnO specimens sintered at 1100 °C for 1 h that contain 1.0 mol % Bi_2O_3 and 1.0 mol % (Sb_2O_3 + Cr_2O_3): (a) 0.3 mol % Cr_2O_3, (b) 0.5 mol % Cr_2O_3, (c) 0.7 mol % Cr_2O_3, (d) 1.0 mol % Cr_2O_3. (◆) δ-Bi_2O_3, (●) pyrochlore, (■) α-$Zn_7Sb_2O_{12}$, (❖) $ZnCr_2O_4$.

Pyrochlore was observed clearly in the specimens with 0.3 mol % Cr_2O_3, barely found in those with 0.5 mol % Cr_2O_3 and hardly found in those with 0.7 mol % Cr_2O_3 as shown in Fig. 5. Comparing with the specimens without Cr, the amount of pyrochlore is very small (see Fig. 6) and is independent of cooling rate (see Fig. 7). Therefore, it is believed that unlike β-spinel, α-spinel that contains a significant amount of Cr does not transform to pyrochlore during cooling. For the specimens consisting of ZnO, Bi_2O_3 and Cr_2O_3, $ZnCr_2O_4$ as well as ZnO and δ-Bi_2O_3 phases were found as shown in Fig. 5d.

The morphology and location of second phases were quite different among the specimens containing Sb_2O_3, both Sb_2O_3 and Cr_2O_3 and Cr_2O_3 only as shown in Fig. 8. For the specimens consisting of ZnO, Bi_2O_3 and Sb_2O_3, spinels, located mostly at the grain

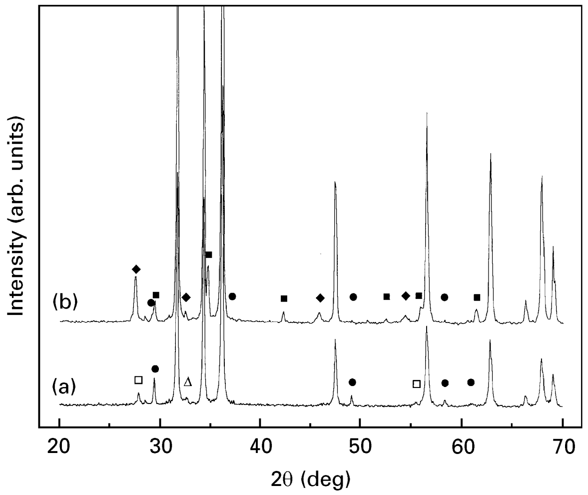

Figure 6 XRD patterns of ZnO specimens sintered at 1100 °C for 1 h that contain 1.0 mol % Bi_2O_3, 0.5 mol % Sb_2O_3: (a) without Cr_2O_3, (b) with 0.5 mol % Cr_2O_3. (■) α-$Zn_7Sb_2O_{12}$, (△) β-$Zn_7Sb_2O_{12}$, (□) β-Bi_2O_3 (●) pyrochlore, (◆) δ-Bi_2O_3.

boundaries, were about 3 μm or larger in size and surrounded by pyrochlore phase as shown in Fig. 8a [12, 14]. On the contrary the specimens consisting of ZnO, Bi_2O_3, Sb_2O_3 and Cr_2O_3 had spinels of 1–2 μm size within grains and at the grain boundaries as shown in Fig. 8b. The second phase, $ZnCr_2O_4$, observed in the specimens containing ZnO, Bi_2O_3 and Cr_2O_3 were less than 1 μm and located at the grain boundaries as aggregates as shown in Fig. 8c. The cause of the size reduction in Cr-containing specimens shown in Fig. 4 was investigated using the contiguity of the grains obtained from Equation 1 and the measurement of the number of interceptions per unit length of test line with ZnO/ZnO and ZnO/liquid phase interface traces. The grain growth during liquid phase sintering is significantly affected by the character of the liquid phase, especially wettability to the solid grains [15]. Although the wettability can be best expressed by the dihedral angle of the liquid phase at the area of ZnO/ZnO grain boundary, direct measurement from the micrograph is very difficult. The contiguity, however, is relatively easy to measure and safely represents the wettability of the liquid phase [15]. Therefore we measured the contiguity of ZnO grains for the specimens with 1.0 mol % Bi_2O_3 and 1.0 mol % Sb_2O_3, and for those with 1.0 mol %Bi_2O_3, 0.5 mol % Sb_2O_3 and 0.5 mol % Cr_2O_3. The contiguities were 0.68 for the former and 0.83 for the latter

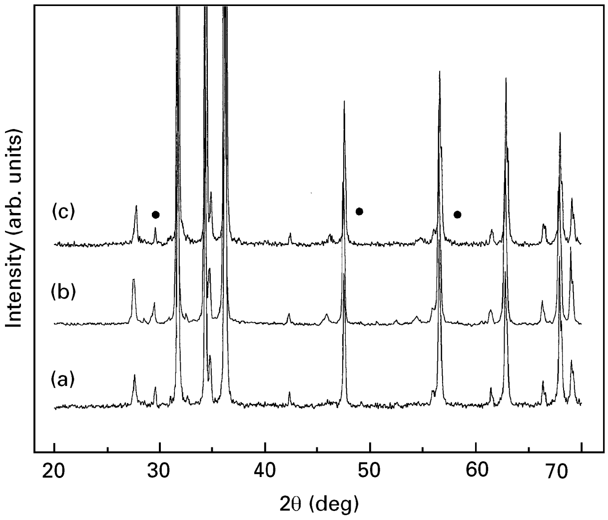

Figure 7 XRD patterns of ZnO specimens sintered at 1100 °C for 1 h that contain 1.0 mol % Bi_2O_3 0.5 mol % Sb_2O_3 and 0.5 mol % Cr_2O_3 prepared under different cooling conditions: (a) slow cooling (2 °C min^{-1}), (b) furnace cooling, and (c) quenching. (●) pyrochlore.

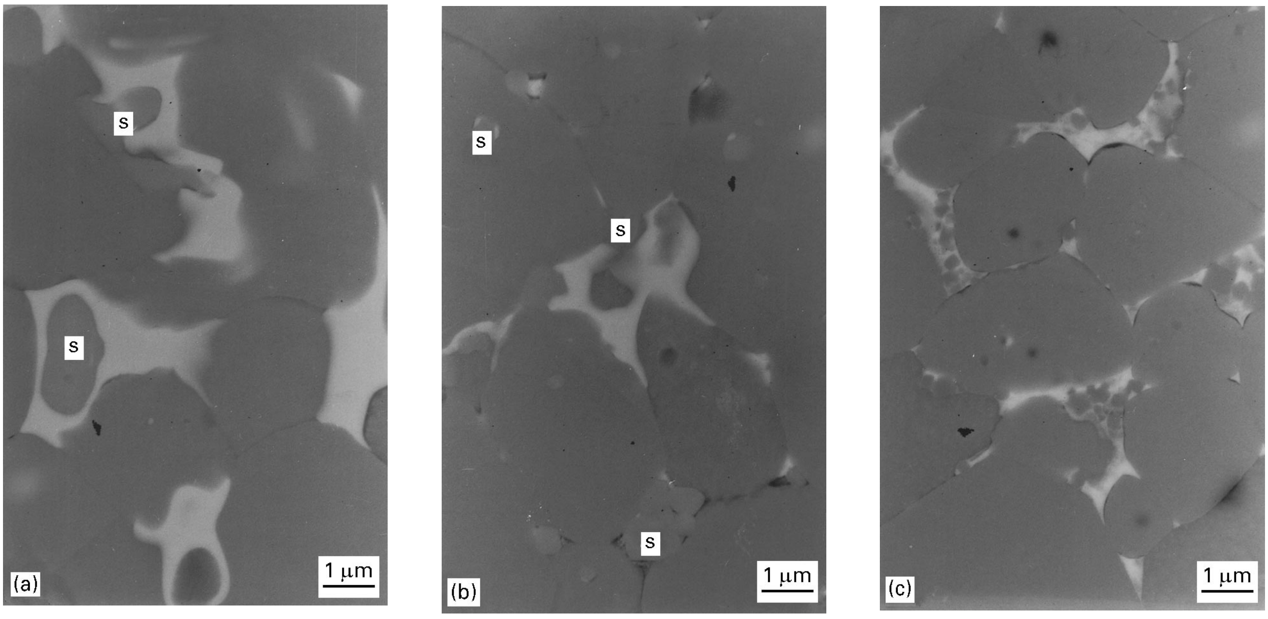

Figure 8 SEM micrograph (back scattered image) of ZnO specimens sintered at 1100 °C for 1 h that contain (a) 1.0 mol % Bi_2O_3 and 1.0 mol % Sb_2O_3, (b) 1.0 mol % Bi_2O_3, 0.5 mol % Sb_2O_3 and 0.5 mol % Cr_2O_3, (c) 1.0 mol % Bi_2O_3 and 1.0 mol % Cr_2O_3. The letter (s) denotes spinel and the bright phase is mostly pyrochlore in (a) and (b), while dark particles in the grain boundary phase are $ZnCr_2O_4$ and bright matrices are the Bi-rich phase in (c).

by counting 200 and 300 grain boundaries, respectively. Because a larger value in contiguity means a lower wettability of the liquid phase to the ZnO grains during sintering, it is believed that the chromium dissolved in the liquid phase lowered the wettability, resulting in reduced grain growth. Further reduction of grain size by addition of Cr was also observed in $ZnO–Bi_2O_3–CoO–Sb_2O_3–Cr_2O_3$ [12].

4. Conclusions

The effect of Cr_2O_3 on the phase formation and microstructure of a ZnO varistor with a basic composition ZnO, Bi_2O_3 and Sb_2O_3 was examined. For specimens consisting of ZnO, Bi_2O_3 and Sb_2O_3, β-spinel was stable at the sintering temperature and transformed to pyrochlore during cooling. On the contrary, for Cr-containing specimens α-spinel was stable at the sintering temperature and hardly transformed to pyrochlore during cooling, irrespective of cooling conditions. For the specimens consisting of ZnO, Bi_2O_3 and Cr_2O_3, $ZnCr_2O_4$ and δ-Bi_2O_3 phases were detected besides ZnO.

When a part of the Sb_2O_3 content was replaced by Cr_2O_3, α-spinel particles of 1–2 μm size that contained a significant amount of Cr were observed within grains and at the grain boundaries. These α-spinel particles were generally smaller than the β-spinel observed in the specimens without Cr and were more effective in grain-growth inhibition. When Sb_2O_3 was completely replaced by Cr_2O_3, aggregates of $ZnCr_2O_4$ particles, smaller than 1 μm, were found at the grain boundaries. The degree of contact, the contiguity, of ZnO grains for the specimens containing Cr was larger than those without Cr, suggesting lower wettability of the liquid phase during sintering for the Cr-containing samples. Therefore it seemed that the addition of Cr changed the nature of the liquid phase during sintering, resulting in reduction of ZnO grain size.

References

1. M. MATSUOKA, *Jpn. J. Appl. Phys.* **10** (1971) 736.
2. T. K. GUPTA, *J. Amer. Ceram. Soc.* **73** (1990) 1817.
3. G. D. MAHAN, L. M. LEVINSON and H. R. PHILIPP, *J. Appl. Phys.* **50** (1979) 2799.
4. M. INADA, *Jpn, J. Appl. Phys.* **19** (1980) 409.
5. J. WONG, *J. Appl. Phys.* **51** (1980) 4453.
6. J. KIM, T. KIMURA and T. YAMAGUCHI, *J. Amer, Ceram, Soc.* **72** (1989) 1541.
7. *Idem, J. Mater. Sci.* **24** (1989) 2581.
8. T. SENDA and R. C. BRADT, *J. Amer, Ceram, Soc.* **74** (1991) 1296.
9. J. KIM, T. KIMURA and T. YAMAGUCHI, *ibid.* **72** (1989) 1390.
10. J. WONG, *J. Appl. Phys.* **46** (1975) 1653.
11. E. E. UNDERWOOD, "Quantitative stereology" (Addison-Wesley, Reading,1970) p. 100.
12. K.-N. KIM and S.-M. HAN, *J. Korean Ceram. Soc.* **28** (1991) 160.
13. H. KANAI and M. IMAI, *J. Mater. Sci.* **23** (1988) 4379.
14. E. OLSSON, L. K. L. FALK, G. L. DUNLOP and R. WESTERLUND, *ibid.* **20** (1985) 4091.
15. D. S. BUIST, B. JACKSON, I. M. STEPHENSON, W. F. FORD and J. WHITE, *Trans. Brit. Ceram. Soc.* **64** (1965) 173.

Received 19 April 1996
and accepted 28 February 1997